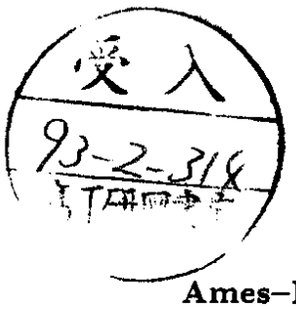

January 1993

Evidence for $f_2(1720)$ Production in the Reaction Pomeron–Pomeron $\to \pi^+\pi^-\pi^+\pi^-$

Ames–Bologna–CERN–Dortmund–Heidelberg–Warsaw Collaboration

A. Breakstone[1*], R. Campanini[2], H.B. Crawley[1], G.M. Dallavalle[2], M.M. Deninno[2], K. Doroba[6], D. Drijard[3], F. Fabbri[2], A. Firestone[1], H.G. Fischer[3], H. Frehse[3**], W. Geist[3***], G. Giacomelli[2], R. Gokieli[6], M. Gorbics[1†], P. Hanke[5], M. Heiden[3††], W. Herr[5†††], L.D. Isenhower[1°], E.E. Kluge[5], J.W. Lamsa[1], R.A. Leacock[1], T. Lohse[4†††], R. Mankel[4], W.T. Meyer[1], G. Mornacchi[3], T. Nakada[5°°], M. Panter[3°°°], A. Putzer[5], K. Rauschnabel[4], B. Rensch[5], F. Rimondi[2], M. Schmelling[4‡], G.P. Siroli[2], J.D. Skeens[1‡‡], R. Sosnowski[6], M. Szczekowski[6], O. Ullaland[3], D. Wegener[4], and R. Yeung[3‡‡‡]

1 Ames Laboratory and Physics Department, Iowa State Univ., Ames, USA
2 Istituto di Fisica dell'Università and INFN, Bologna, Italy
3 CERN, European Organization for Nuclear Research, Geneva, Switzerland
4 Institut für Physik der Universität, Dortmund, Germany
5 Institut für Hochenergiephysik, Heidelberg, Germany
6 University and Institute for Nuclear Research, Warsaw, Poland

Submitted to Zeitschrift für Physik C

---

*	Present address:	University of Hawaii, USA
**	Present address:	CONVEX, Zürich, Switzerland
***	Present address:	CRN Strasbourg, France
†	Present address:	LeCroy Research Systems, Chestnut Ridge, NY, USA
††	Present address:	DEC, Kaufbeuren, Germany
†††	Present address:	CERN, Geneva, Switzerland
°	Present address:	Abilene Christian University, Texas, USA
°°	Present address:	Paul Scherer Institute, Villigen, Switzerland
°°°	Present address:	Max Planck Institute, Heidelberg, Germany
‡	Present address:	University of Mainz, Germany
‡‡	Present address:	Rice University, Houston, Texas, USA
‡‡‡	Present address:	CALTECH, Pasadena, California, USA

ABSTRACT

Data are presented on Pomeron-Pomeron interactions which produce a central $\pi^+\pi^-\pi^+\pi^-$ system in proton-proton collisions at $\sqrt{s} = 62$ GeV at the CERN Intersecting Storage Rings. A spin-parity analysis of the $\pi^+\pi^-\pi^+\pi^-$ system shows evidence for the production of the state $f_2(1720)$ with decay to $\rho^0\pi^+\pi^-$. Since Pomeron-Pomeron interactions are expected to favor the production of gluonic bound states, observation of the $f_2(1720)$ supports earlier interpretations of it as a glueball. In addition, enhancements near threshold give indication of the state $f_2(1270)$ decaying to $\rho^0\rho^0$ and the state $f_0(1400)$ decaying to $\rho^0\pi^+\pi^-$.

1. Introduction

We present a study of Double-Pomeron-Exchange (DPE) from the reaction

$$p\,p \to p\,p\;\pi^+\pi^-\pi^+\pi^- \tag{1}$$

at a center-of-mass energy $\sqrt{s} = 62$ GeV. Pomeron-Pomeron (**PP**) interactions are obtained by selecting two diffractively scattered protons at large Feynman-x plus a centrally produced system. The exchanged Pomerons produce the reaction

$$\mathbf{P}\,\mathbf{P} \to \pi^+\pi^-\pi^+\pi^- \tag{2}$$

as shown in Fig. 1. The Pomeron, **P**, is generally assumed to be a multi-gluon state with the quantum numbers of the vacuum [1]. Pomeron-Pomeron interactions can produce only $I=0$ states with $J^{PC} = 0^{++}$, 2^{++}, 4^{++}, etc. The production of glueball states is expected to be enhanced as a result of the high gluonic content of the **PP** interaction. Previous work by this collaboration on inclusive **PP** interactions and on the reaction $\mathbf{P}\,\mathbf{P} \to \pi^+\pi^-$ can be found in Ref. 2.

2. Data Acquisition and Selection

The Intersecting Storage Rings (ISR) at CERN provided good conditions for the study of reaction (1) because of their high luminosity and open geometry. Data were taken at $\sqrt{s} = 62$ GeV with the Split-Field-Magnet (SFM) detector [3], which had a 1 Tesla field and excellent solid-angle coverage (~95%) for charged particles. It was composed of multiwire proportional chambers (MWPC) arranged into a central detector plus two forward telescopes along the outgoing beams.

The trigger required a fast charged particle in each forward telescope, plus at least one charged particle in the central region. Included was a veto on charged particles produced at intermediate polar angles. The integrated luminosity was 50 nb^{-1}.

Events satisfying the trigger conditions were processed with standard SFM reconstruction codes. Events with one positive forward track ($| x_f | > 0.7$) in each of the two telescopes and four central tracks ($| x_f | < 0.3$), two positive and two negative, were selected. In order to reject events with additional neutral particles and to assign the correct hypothesis, the selected events were subjected to a four-constraint kinematic fit. Background from other channels is estimated to be less than 15%. A study of contamination from $2\pi^0$ states was made by randomly removing a charged pion pair from the six-charged-pion four-constraint fitted reactions and then attempting a fit to reaction (1). We point out that contamination from the reaction with four charged pions plus one π^0 should be very small since an odd number of pions is forbidden for double-Pomeron-exchange. The final data sample consists of 5800 events.

In previous work we published evidence that, in the above trigger configuration, reaction (1) is dominated by Double-Pomeron-Exchange [2]. In addition, a cross-section of $\simeq 46$ μb for DPE was determined for reaction (1).

3. Acceptance Corrections

Acceptances have been calculated using Monte-Carlo techniques. Complete events were generated using a double-peripheral model [4]. Peripheral production of the outgoing protons was simulated by using the matrix-element squared $\exp(A\,t_1)\cdot\exp(A\,t_2)$, where t_1 and t_2 are the four-momentum-transfers squared from initial to final-state protons and with $A \simeq 6$. A gaussian p_T-damping with respect to the Pomeron direction was used for the 4π decay of the central system. The t distribution of the protons and the p_T distribution of the pions produced from this model agree with the data. Particle trajectories were tracked through the magnetic field and the detector chambers [5]. Energy losses, scattering, and particle decays were included. Further details of the calculation may be found in Ref. 2.

Trigger requirements were imposed on the Monte-Carlo data and combined with the SFM reconstruction efficiency in order to obtain the full acceptance. The calculation was done for 0.1 GeV intervals of the $\pi^+\pi^-\pi^+\pi^-$ invariant mass. The acceptance ranges from 0.002 to 0.003 over the $\pi^+\pi^-\pi^+\pi^-$ mass range 1.2 to 4.0 GeV (see Ref. 2). Variations of 10 to 15% result when matrix-elements for different J^P states (Section 4) are included in the calculation. We note that a large fraction (95%) of the acceptance correction results from the trigger requirement for the forward protons.

4. Analysis of the $\pi^+\pi^-\pi^+\pi^-$ System

The $\pi^+\pi^-\pi^+\pi^-$ invariant mass distribution, $M(4\pi)$, corrected for acceptance, is shown in Fig. 2 for the events of reaction (1). The mass distribution features a rapid rise from threshold to the 1300 MeV region. In addition, there is a broad enhancement which peaks near 1750 MeV. The $\pi^+\pi^-$ invariant mass distribution exhibits a clear ρ^0 signal, which is treated in the analysis that follows. The $\pi^\pm\pi^\pm\pi^\mp$ invariant mass distribution (not shown) has no indication for resonance production of three-pion states.

We have examined the moments of spherical harmonics, $\langle Y_m^l(\cos\theta,\phi)\rangle$, for the decay of the 4π system to two $\pi^+\pi^-$ pairs with orbital angular momentum L, and for the decay of the $\pi^+\pi^-$ subsystems (orbital angular momentum l). Orbital angular momenta $L, l = 0$ or 1 with $m = 0$ were sufficient to describe the moments for $M(4\pi) < 3.0$ GeV. We therefore make the assumption that, for **PP** interactions, the dominant contributions to our data are from $J^P = 0^+, 2^+$ $(m = 0)$ states. A thorough study of the evidence which substantiates the dominance of DPE in reaction (1) may be found in Ref. 2.

We follow the general procedure first applied in the reaction $\gamma\gamma \to \pi^+\pi^-\pi^+\pi^-$ [6]. The production cross-section is taken as

$$d\sigma/d\xi \propto |g_i(\xi)|^2 \, W_4(\xi)$$

where $g_i(\xi)$ is the matrix element for a particular production mechanism (i), describing resonance formation and decay angular correlations, and $W_4(\xi)$ is four-pion phase space. The cross-section depends on seven independent variables represented as

$$\xi = (m_{12}^2,\, m_{34}^2,\, \theta_{12},\, \vartheta_{12}^\pi,\, \varphi_{12}^\pi,\, \vartheta_{34}^\pi,\, \varphi_{34}^\pi)\,.$$

The pions are labeled as $\pi_1^+, \pi_2^-, \pi_3^+, \pi_4^-$; m_{ij} is the invariant mass of π_i^+ and π_j^-; θ_{12} is the polar angle of pion pair $(1,2)$ with respect to the **PP** axis in the four-pion cms, and ϑ_{ij}^π , φ_{ij}^π are the polar and azimuthal angles of the π^+ in the $\pi^+\pi^-$ rest frame with respect to the **PP** axis in the four-pion cms. There are two combinations per event.

A maximum-likelihood fit was performed to determine the contributions of the particular production mechanisms being considered [7]. The likelihood function for an incoherent sum, used in the next section to determine the amount of ρ^0 production, is defined as

$$L = \prod_n \sum_i a_i \, P_i(\xi_n)$$

with $\Sigma\, a_i = 1$, where a_i is the fractional contribution of process (i), described by g_i. The product is over the events in a given 4π mass interval, and the sum is over the production contributions considered. $P_i(\xi_n)$ is the probability for an event n with variables ξ_n to

be produced by production mechanism (i). Each contribution is normalized such that its integral over the acceptance is unity.

$$P_i(\xi) = A(\xi)\,(d\sigma_i(\xi)/d\xi) \Big/ \int A(\xi)\,d\sigma_i(\xi)$$

where $A(\xi)$ is the acceptance for an event with variables ξ. The integrals over the acceptance were calculated with Monte-Carlo procedures (as in Section 3). Monte-Carlo events were weighted with the various matrix-elements $\mid g_i \mid^2$, and trigger and detector acceptances were imposed. In the definition of the likelihood function, the phase space $W_4(\xi)$ and the acceptance $A(\xi)$ were factored out since they are the same for all processes. The maximization was performed on the logarithm of the likelihood function.

For the case of a coherent sum of amplitudes the likelihood function is correspondingly defined as

$$L = \prod_n \sum_{ij} \sqrt{a_i\,a_j}\,A(\xi)\,g_i(\xi)\,g_j^*(\xi)\,W_4(\xi) \Big/ \int A(\xi)\,g_i(\xi)\,g_j^*(\xi)\,W_4(\xi)\,d\xi$$

where the sum is over all combinations (ij) of the contributions considered. The amplitudes $g(\xi)$, for the coherent case, contain relative phase factors which, in addition to the fractional contributions (a_i), are included as free parameters in the fitting procedure. This method is used in the analysis which follows to combine various spin-parity states.

4.1 ρ^0 Production as a Function of $M(4\pi)$

Preliminary to our spin-parity analysis we attempt to determine, using a straightforward method, the amount of ρ^0 production as a function of $M(4\pi)$. The data are fitted to an incoherent mixture of isotropic $\pi^+\pi^-\pi^+\pi^-$, $\rho^0\pi^+\pi^-$, and $\rho^0\rho^0$ states, without reference to specific spin-parity states. This formulation does not attempt to take into consideration angular momentum and parity conservation. It should be regarded essentially as a fit to the four-dimensional $\pi_i^+\pi_j^-$ invariant-mass distribution. To the extent that the ρ^0 signal can be distinguished from a wider background, this method should provide a reasonable determination of the ρ^0 content ($\rho\pi\pi$ and $\rho\rho$) in the data. The matrix elements g_i , which contain only Breit-Wigner amplitudes and no explicit angular correlations, are

$$g_{4\pi} = 1$$

$$g_{\rho\pi\pi} = (1/2)\left\{BW(m_{12}) + BW(m_{34}) + BW(m_{14}) + BW(m_{23})\right\}$$

$$g_{\rho\rho} = (1/\sqrt{2})\left\{BW(m_{12})\;BW(m_{34}) + BW(m_{14})\;BW(m_{23})\right\}$$

where $BW(m_{ij})$ is the relativistic Breit-Wigner amplitude for the ρ^0, with $m_\rho = 770$ MeV and $\Gamma_\rho = 153$ MeV. The results of the maximum-likelihood fit for the decomposition

into components 4π , $\rho\pi\pi$, and $\rho\rho$ as a function of $M(4\pi)$ are shown in Table 1. A $\rho\rho$ enhancement is seen in the data from threshold to 1400 MeV, comprising 30% of the cross-section in that region $\star$. The $\rho\pi\pi$ component rises slowly to a broad enhancement, reaching 40% of the cross-section in the 1800 MeV region. The direct 4π contribution is relatively constant with respect to $M(4\pi)$. In addition, below 1600 MeV, there is a negative correlation between the fitted $\rho\pi\pi$ and $\rho\rho$ amounts, which produces larger errors for those terms. However, the combined ρ^0 contributions (sum of $\rho\pi\pi$ and $\rho\rho$) are better determined, as is indicated by the errors of their complement, the direct 4π terms. The ρ^0 content obtained here will be used as a constraint in the fitting procedure for the spin-parity analysis which follows.

4.2 Spin-Parity Composition of the 4π , $\rho\pi\pi$, and $\rho\rho$ States

We now attempt to determine the spin-parity composition of the 4π , $\rho\pi\pi$, and $\rho\rho$ states as a function of $M(4\pi)$. Matrix-elements are defined which contain angular correlations corresponding to specific spin and parity. Neglecting spins of 4 or greater we consider $J^P = 0^+, 2^+$.

The rotational properties of the matrix-elements can be described as a sum of products of three spherical harmonics as

$$\Psi^{J^P} \propto \Sigma\, a^{J^P}_{L,L_Z,l_{12},l_{34},S_{12},S_{34}}\; Y_L^{L_Z}(\theta_{12},\phi_{12})\; Y_{l_{12}}^{S_{12}}(\vartheta^{\pi}_{12},\varphi^{\pi}_{12})\; Y_{l_{34}}^{S_{34}}(\vartheta^{\pi}_{34},\varphi^{\pi}_{34})$$

where the $\pi^+\pi^-$ pairs are (1,2) and (3,4). The sum is over L and L_Z, the orbital angular momentum and its projection between the two $\pi^+\pi^-$ pairs, and l_{ij} and S_{ij}, the orbital angular momentum and its projection within a $\pi^+\pi^-$ pair. The dependence on ϕ_{12} is integrated out. The production angular distribution of a $\pi^+\pi^-$ pair is described by $Y_L^{L_Z}$ and the decay distribution of the pair by $Y_{l_{ij}}^{S_{ij}}$. The production and decay angles are defined with respect to the **PP** axis in the 4π cms and $\pi^+\pi^-$ cms, respectively. The coefficients $a^{J^P}_{L,L_Z,l_{12},l_{34},S_{12},S_{34}}$ are derived with the condition $L, l_{ij} = 0$, 1 or 2. This results in a total of 13 different matrix-elements: seven for the direct 4π state, four for the $\rho\pi\pi$ state, and two for the $\rho\rho$ state. In the above, $L + l_{12} + l_{34} \geq 4$ is neglected. For definite spin-parity states, the $g(\xi)$ are:

$$g^{J^P}_{4\pi} = \Psi^{J^P}(\theta_{12},\, \vartheta^{\pi}_{12},\, \varphi^{\pi}_{12},\, \vartheta^{\pi}_{34},\, \varphi^{\pi}_{34}) + \Psi^{J^P}(\theta_{14},\, \vartheta^{\pi}_{14},\, \varphi^{\pi}_{14},\, \vartheta^{\pi}_{23},\, \varphi^{\pi}_{23})$$

$$g^{J^P}_{\rho\pi\pi} = (1/2)\,\{BW(m_{12})\;\Psi^{J^P}(\theta_{12},\, \vartheta^{\pi}_{12},\, \varphi^{\pi}_{12},\, \vartheta^{\pi}_{34},\, \varphi^{\pi}_{34}) + [\text{ 3 permutations }]$$

$\star$ Similar enhancements seen below nominal $\rho\rho$ threshold have been reported in the reaction $\gamma\gamma \to \pi^+\pi^-\pi^+\pi^-$, for example, see Ref. 6.

$$g_{\rho\rho}^{J^P} = (1/\sqrt{2})\,\{BW(m_{12})\,BW(m_{34})\;\Psi^{J^P}(\theta_{12},\,\vartheta_{12}^{\pi},\,\varphi_{12}^{\pi},\,\vartheta_{34}^{\pi},\,\varphi_{34}^{\pi})$$
$$+BW(m_{14})\,BW(m_{23})\;\Psi^{J^P}(\theta_{14},\,\vartheta_{14}^{\pi},\,\varphi_{14}^{\pi},\,\vartheta_{23}^{\pi},\,\varphi_{23}^{\pi})\}$$

Maximum-likelihood fits involving various sets of the different matrix-elements up to the full number of 13 were performed for 0.1 GeV intervals of the 4π mass spectrum. Only five matrix-elements were found to yield contributions which were larger than a few percent and not consistent with zero. These five matrix-elements comprise one direct 4π term ($J, L, l = 0$, phase space), two $\rho\pi\pi$ terms ($J = 0, 2$ with $L = 0$), and two $\rho\rho$ terms ($J = 0, 2$). Even with this minimal set of matrix-elements the errors on the $\rho\pi\pi$ and $\rho\rho$ contributions were unacceptably large. In an attempt to reduce the fitted errors and thereby obtain more conclusive results on the spin-parity composition of the data, we added a constraint on the amount of ρ^0 which is allowed to be fitted as a function of $M(4\pi)$. The total amount of ρ^0 ($\rho\pi\pi$ and $\rho\rho$) fitted previously (in Section 4.1) with the Breit-Wigner matrix-elements was used to provide a constraint for a fit using the above five matrix-elements. In the fits without this constraint we obtained about 30% less ρ^0 contribution, but it was consistent within errors to the present fit. As a caveat, we point out that in principle there is an additional uncertainty in these results due to the necessity to include only a relatively small number of terms in the partial wave analysis. This is common to most partial wave analyses, but may be particularly important in many particle final states.

The results of the above fit are shown in Fig. 3a-e. A strong signal can be seen in the $J = 2$ $\rho\pi\pi$ mass spectrum (Fig. 3d) at 1750 MeV. In addition there are enhancements near 1300 MeV in the $J = 0$ $\rho\pi\pi$ and $J = 2$ $\rho\rho$ mass spectra, Figs. 3b and 3e. The results of the fits for the phase angles, which have large errors, do not indicate any pattern and are not shown. The fit in the 1750 MeV region yields only one large contribution, namely $J^P = 2^+$ $\rho\pi\pi$, in addition to that from the direct 4π $J = 0$ state. We examine this region in more detail below.

The quality of the fit for the mass range $1.7 < M(4\pi) < 1.9$ GeV can be seen from the distribution of $M(\pi^+\pi^-)$ and the angular distributions $\cos(\vartheta_\pi)$ and $\Delta\varphi$, shown in Figs. 4-6. ϑ_π is the polar angle of a pion with respect to the **PP** axis in the $\pi^+\pi^-$ cms. $\Delta\varphi$ is the angle between the decay planes for the two $\pi^+\pi^-$ systems in the 4π cms. The curves on the figures representing the results of the fit are obtained using Monte-Carlo simulation. The fitted parameters are used in the Monte-Carlo matrix elements, and the effects of the experimental acceptance are included. Figure 4a shows the distribution of $M(\pi^+\pi^-)$ for the 4π mass range studied. To illustrate better the contribution of ρ^0 production, Fig. 4b displays the data and fit after subtraction of the direct 4π $J = 0$ contribution. Figs. 5a and 6a show, for the same 4π mass range, the distributions $\cos(\vartheta_\pi)$ and $\Delta\varphi$ along with the

fit. The structure of these distributions after subtraction of the direct 4π contribution is shown in Figs. 5b and 6b. The dashed and solid curves in this case are predictions for pure $\rho\pi\pi$ $J = 0$ and $J = 2$ states, respectively. As seen in Fig. 6b, the $J = 2$ prediction provides better agreement with the data.

We summarize briefly the evidence for the $f_2(1720)$ from selected previous experiments. The $f_2(1720)$ has been seen in the $K\bar{K}$ system from 'gluon rich' J/ψ radiative decay, although without conclusive spin-parity determination [8,9,10]. In Ref. 10, spin 0 is preferred, however an additional spin 2 state is also possible. The $K\bar{K}$ signal is also seen by the WA76 collaboration in 300 GeV pp central production with $J^P = 2^+$ strongly favored [11]. In addition, a four-pion decay mode $\pi^0\pi^0\pi^0\pi^0$ with evidence for $J^P = 2^+$ is reported by the GAMS collaboration [12].

We identify the signal at 1750 MeV seen in this experiment with the $f_2(1720)$ signals reported above. We have not attempted to fit the mass and width of the 1750 MeV state because of the difficulty in choosing an appropriate background. The resonance parameters and cross-sections in Table 2 are estimated using hand-drawn backgrounds. Even for the experiments quoted above, sharply rising or falling backgrounds added to (or multiplied by) Breit-Wigner resonance shapes have made mass and width determinations uncertain. In addition to dependence on background assumptions, interference with nearby resonances adds to the difficulty. The decay mode seen in this experiment, $f_2(1720) \rightarrow \rho\pi\pi$, is reported for the first time. We have no evidence for a decay in either the direct 4π or $\rho\rho$ modes. The $4\pi^0$ decay mode (note $\rho^0 \not\rightarrow \pi^0\pi^0$) seen in the GAMS experiment [12] occurs with a very small cross-section and is not incompatible with our result.

The enhancements near 1300 MeV seen in both the $J = 0$ and $J = 2$ components, Figs. 3b and 3e, may be identified with the states $f_0(1400)$ and $f_2(1270)$, respectively. By comparing the cross-sections found in this experiment (Table 2) with those from Ref. 2 we find the branching ratios $\pi^+\pi^-\pi^+\pi^-/\pi^+\pi^-$ for the $f_0(1400)$ and $f_2(1270)$ to be $0.05 \leftrightarrow 0.10$ and $0.09 \leftrightarrow 0.18$, respectively. The branching ratio for the $f_2(1270)$ is at least twice as large as that reported by the Particle Data Group [8]. A branching ratio which is process dependent is possible should the $f_2(1270)$ be composed of an f-glueball mixture [13]. We note that indication of a glueball mixture for the $f_2(1270)$ has been previously suggested in Ref. 2.

5. Conclusions

Data have been presented on the production of $\pi^+\pi^-\pi^+\pi^-$ systems in the central region from Pomeron-Pomeron reactions in proton-proton collisions at 62 GeV at the CERN Intersecting Storage Rings. The $\pi^+\pi^-\pi^+\pi^-$ mass spectrum exhibits a rapid rise from threshold to the 1300 MeV region, and an enhancement near 1750 MeV. The 1300 MeV region is comprised equally of $J^P = 2^+$ $\rho\rho$ and $J^P = 0^+$ $\rho\pi\pi$ contributions, attributable to decay modes of the states $f_2(1270)$ and $f_0(1400)$, respectively. The 1750 MeV enhancement, with $J^P = 2^+$, can be identified with the $f_2(1720)$ decaying to $\rho^0\pi^+\pi^-$. Observation of this state in gluon rich **PP** interactions strenghtens its interpretation as a glueball.

Acknowledgments

We are grateful for the support provided by the SFM detector group and the ISR Experimental Support group. The Dortmund and Heidelberg groups were supported by a grant from the Bundesministerium für Forschung und Technologie of the Federal Republic of Germany. The Ames group was supported by the U.S. Department of Energy under contract W-7405-ENG-82.

References

[1] F.E. Low: Phys. Rev. D12 (1975) 163; S. Nussinov: Phys. Rev. D14 (1976) 246; J. Pumplin and E. Lehman: Z. Phys. C - Particles and Fields 9 (1981) 25; P.V. Landshoff and O. Nachtmann: Z. Phys. C - Particles and Fields 35 (1987) 405; A. Donnachie and P.V. Landshoff: Nucl. Phys. B311 (1988/89) 509

[2] A. Breakstone et al.: Z. Phys. C - Particles and Fields 42 (1989) 387; A. Breakstone et al.: Z. Phys. C - Particles and Fields 48 (1990) 569

[3] R. Bouclier et al.: Nucl. Instr. Meth. 115 (1974) 135; R. Bouclier et al.: Nucl. Instr. Meth. 125 (1975) 19; W. Bell et al.: Nucl. Instr. Meth. 156 (1978) 111

[4] F. James: FOWL, CERN, Program Library (1967); E. Byckling, M. Kaartinen, K. Kajantie, and H. Villanen: Res. Inst. Theor. Phys. Report No. 3-69, 1969 (unpublished)

[5] R. Messerli: SFMGENER, CERN (unpublished)

[6] TASSO Coll., M. Althoff et al.: Z. Phys. C - Particles and Fields 16 (1982) 13

[7] F. James and M. Roos: MINUIT, CERN, Program Library (1989)

[8] Particle Data Group: Phys. Lett. 239B (1990) 1

[9] DM2 Coll., J.E. Augustin et al.: Phys. Rev. Lett. 60 (1988) 2238

[10] MARK-III Coll., L.-P. Chen: Nucl. Phys. B (Proc. Suppl.) 21 (1991) 80

[11] WA76 Coll., T.A. Armstrong et al.: Phys. Lett. 227B (1989) 186

[12] IHEP-IISN-LANL-LAPP Coll., D. Alde et al.: Phys. Lett. 198B (1987) 286

[13] J.F. Donoghue, K. Johnson and B.A. Li: Phys. Lett. 99B (1981) 416; J.F. Donoghue: Phys. Rev. D25 (1982) 1875

Table 1. Results of the fit for the decomposition into $\rho\rho$, $\rho\pi\pi$, and 4π as a function of $M(4\pi)$, in 100 MeV bins, as a percent of the cross-section.

$M(4\pi)$	$\rho^0\rho^0$	$\rho^0\pi^+\pi^-$	$\pi^+\pi^-\pi^+\pi^-$
1150	33 ± 12	0 ± 5	67 ± 13
1250	22 ± 12	34 ± 19	44 ± 13
1350	40 ± 10	11 ± 14	49 ± 11
1450	13 ± 8	13 ± 13	74 ± 10
1550	9 ± 7	24 ± 11	67 ± 8
1650	15 ± 8	23 ± 12	62 ± 7
1750	7 ± 8	37 ± 11	56 ± 7
1850	0 ± 5	39 ± 7	61 ± 7
1950	0 ± 3	38 ± 7	62 ± 7
2050	9 ± 7	17 ± 10	74 ± 8
2150	15 ± 6	4 ± 9	81 ± 8
2250	0 ± 5	28 ± 7	72 ± 8
2350	2 ± 7	39 ± 11	59 ± 8
2450	9 ± 7	6 ± 11	85 ± 10
2550	0 ± 8	16 ± 9	84 ± 11
2650	3 ± 8	18 ± 14	79 ± 12
2750	10 ± 7	21 ± 13	69 ± 12
2850	0 ± 3	1 ± 12	99 ± 14
2950	6 ± 8	27 ± 15	67 ± 14

Table 2. Estimated resonance parameters and cross-sections for DPE exclusive reactions, with a 4π decay mode for the resonant states. The cross-sections have a systematic error ($1.5\times$) resulting from an overall acceptance uncertainty and the luminosity calibration.

Reaction	Mass	Width	σ [μb]
(1) $pp \to pp\ (\pi^+\pi^-\pi^+\pi^-)$			46.0
(2) $pp \to pp\ f_2(1270)$	1300	150 to 200	0.7
(3) $pp \to pp\ f_0(1400)$	1300	150 to 200	1.0
(4) $pp \to pp\ f_2(1720)$	1750	200 to 300	2.5

Figure Captions

Fig.1 Double-Pomeron-Exchange diagram. A central $\pi^+\pi^-\pi^+\pi^-$ system is produced from the collision of two Pomerons (**P**).

Fig.2 Invariant mass distribution for the central $\pi^+\pi^-\pi^+\pi^-$ system from reaction (1), in μb per 100 MeV bin. In this and in all subsequent figures the data shown have been corrected for acceptances.

Fig.3 Invariant mass distributions for the central $\pi^+\pi^-\pi^+\pi^-$ system for various spin-parity states as determined from a partial wave decomposition, in μb per 100 MeV bin. (a) 4π $J=0$. (b) $\rho\pi\pi$ $J=0$. (c) $\rho\rho$ $J=0$. (d) $\rho\pi\pi$ $J=2$. (e) $\rho\rho$ $J=2$.

Fig.4 (a) Distribution of the $\pi^+\pi^-$ invariant mass for events in the 4π mass region $1.7 < M(4\pi) < 1.9$ GeV. The curve shows the result of the fit to a sum of spin-parity states, see text. (b) As above after the subtraction of the fitted direct 4π component from the data and from the fitted result.

Fig.5 (a) Distribution of $\cos(\vartheta_\pi)$ for events in the 4π mass region $1.7 < M(4\pi) < 1.9$ GeV. The curve shows the result of the fit, see text. (b) As above after the subtraction of the fitted direct 4π component from the data. The dashed and solid curves, in this case, represent the predictions of pure $\rho\pi\pi$ $J=0$ and $J=2$ states, respectively.

Fig.6 (a) Distribution of $\Delta\varphi$ for events in the 4π mass region $1.7 < M(4\pi) < 1.9$ GeV. The curve shows the result of the fit, see text. (b) As above after the subtraction of the fitted direct 4π component from the data. The dashed and solid curves, in this case, represent the predictions of pure $\rho\pi\pi$ $J=0$ and $J=2$ states, respectively.

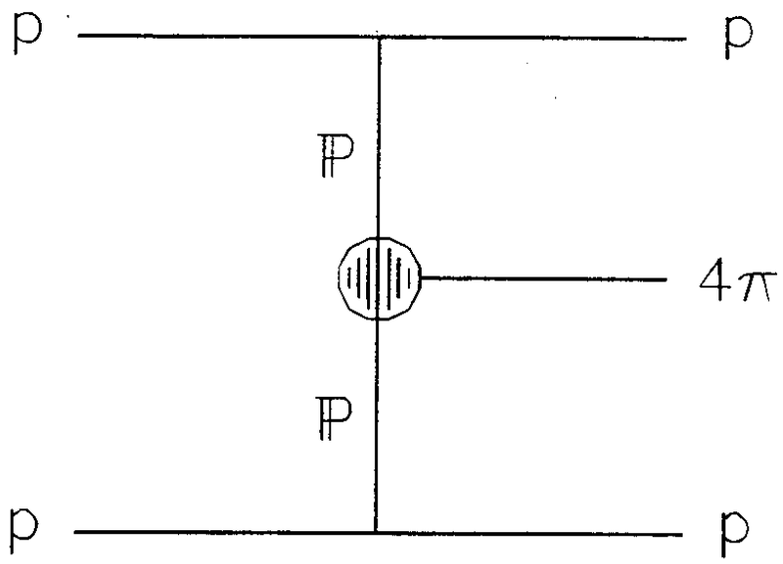
p
p
$\mathbb{P}$
4π
$\mathbb{P}$
p
p

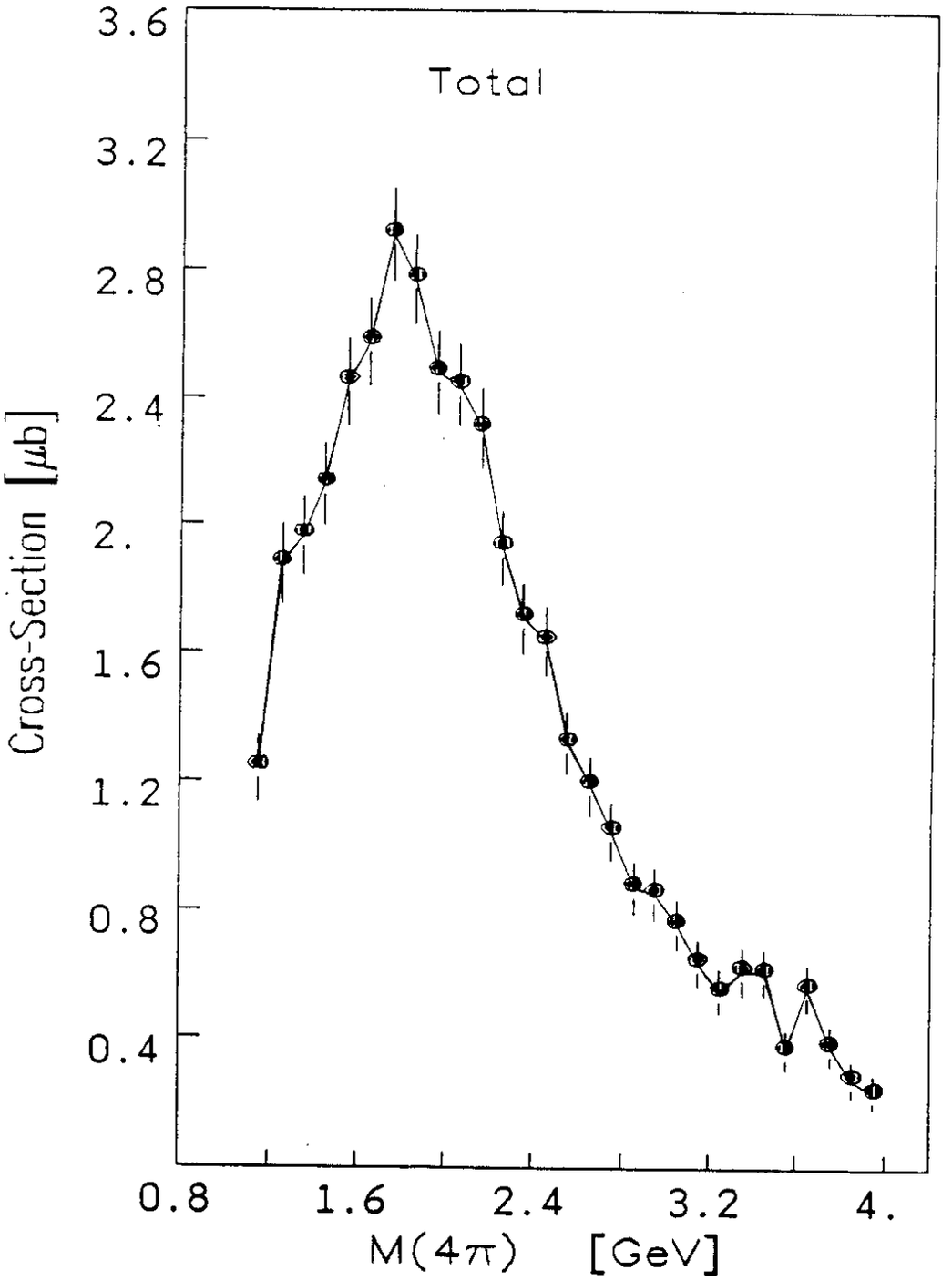
Total
Cross-Section [μb]
3.6
3.2
2.8
2.4
2.
1.6
1.2
0.8
0.4
0.8
1.6
2.4
3.2
4.
M(4π) [GeV]

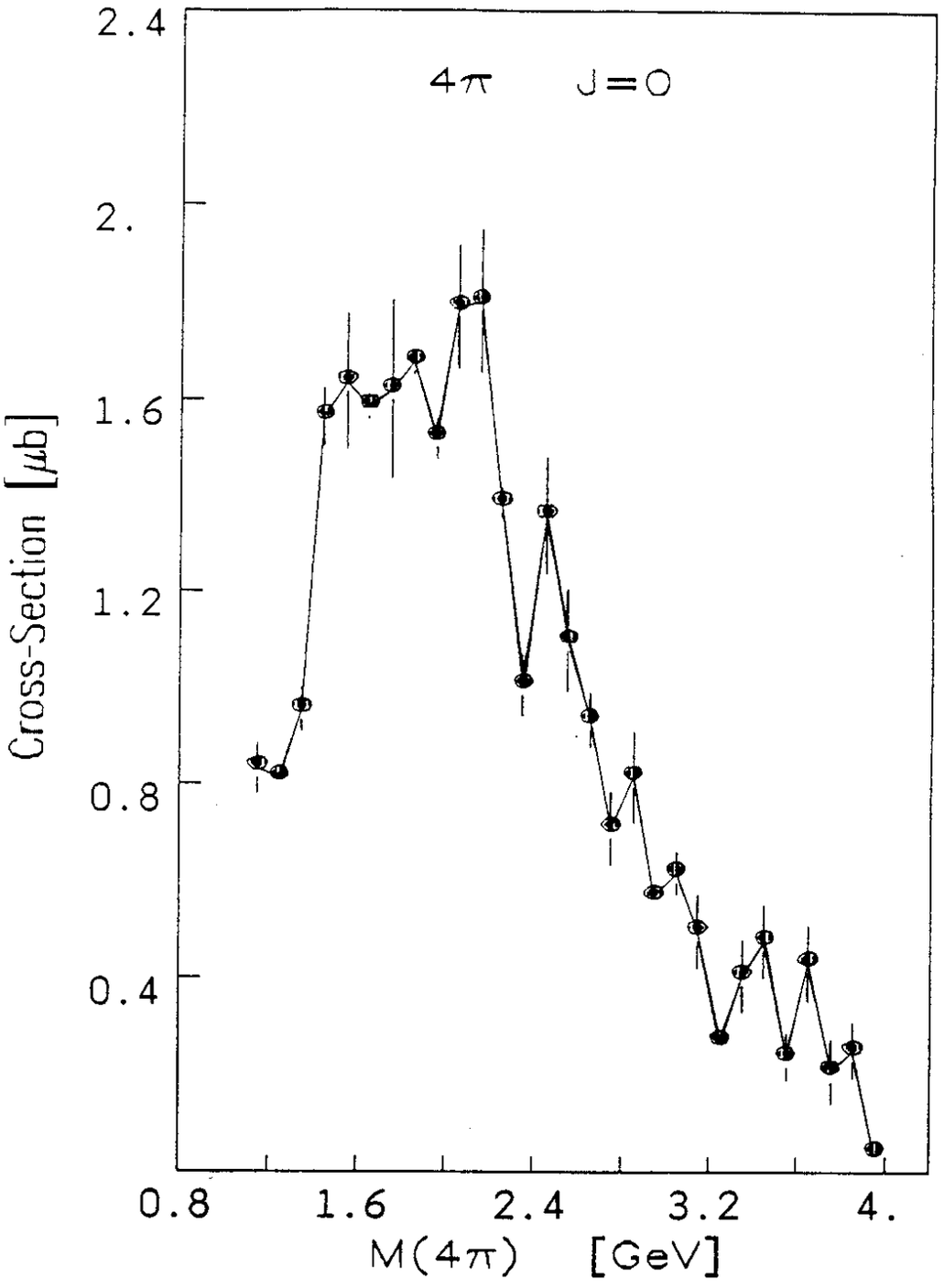

3a

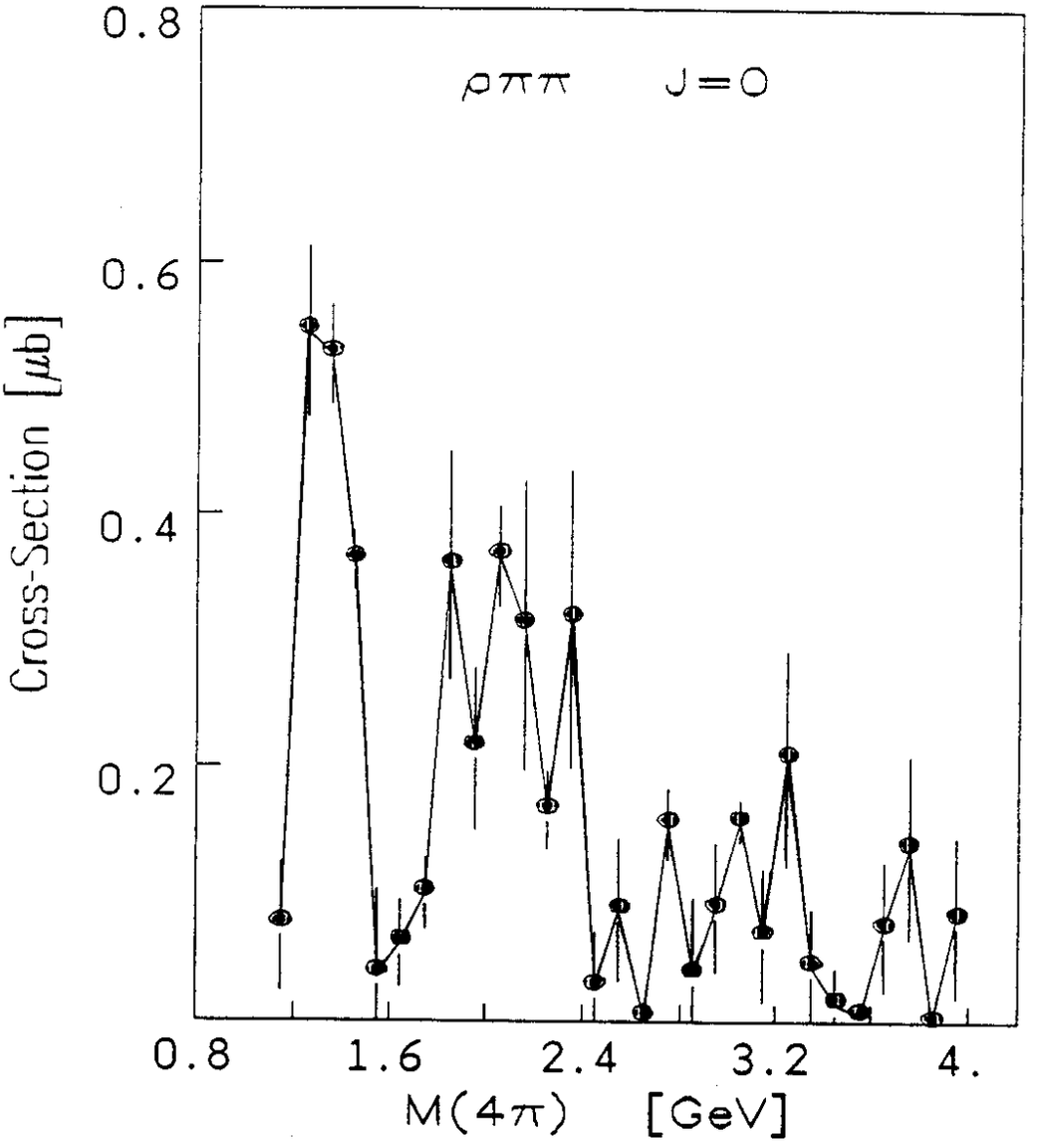

3b

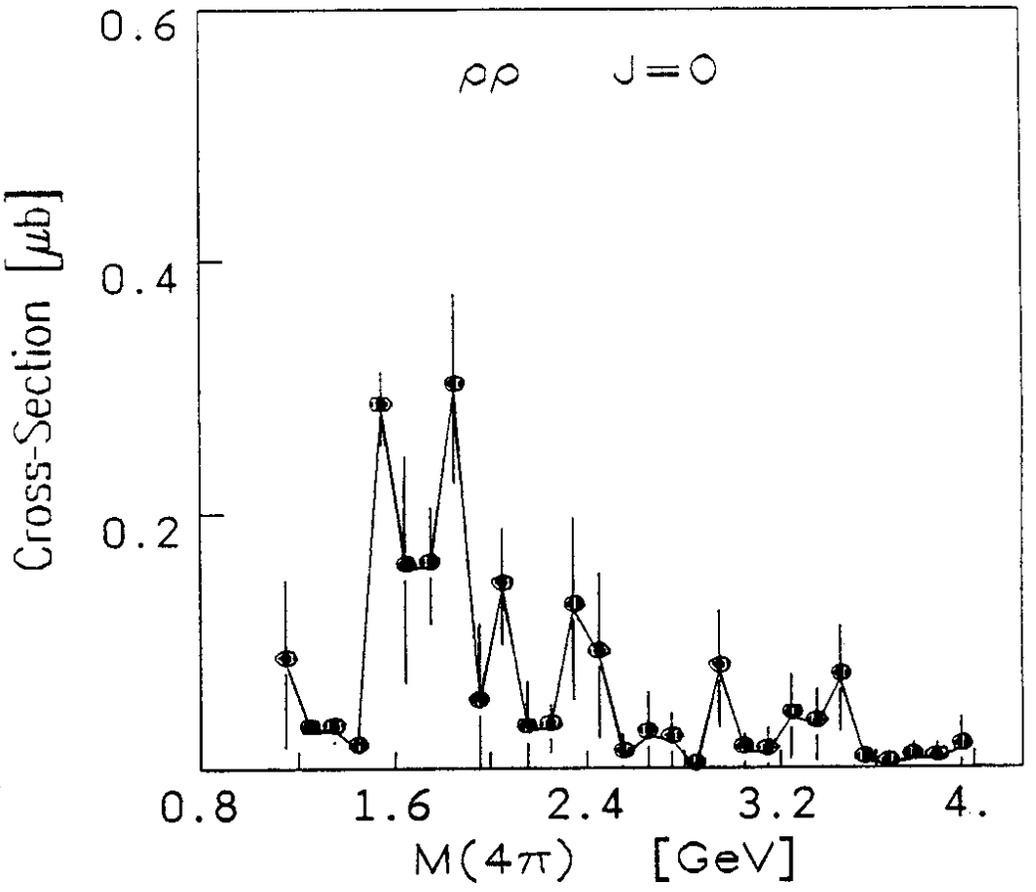

3c

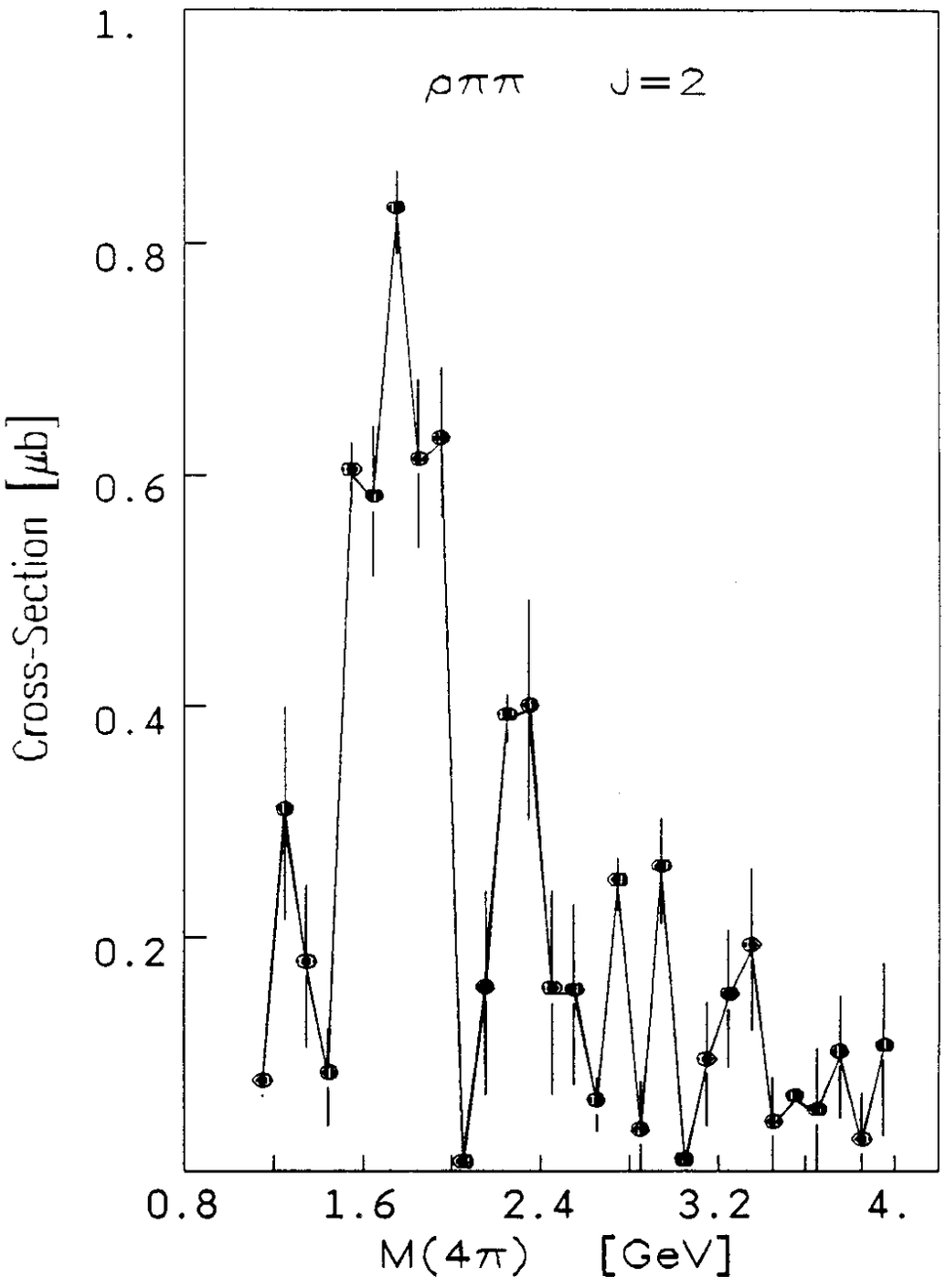

3d

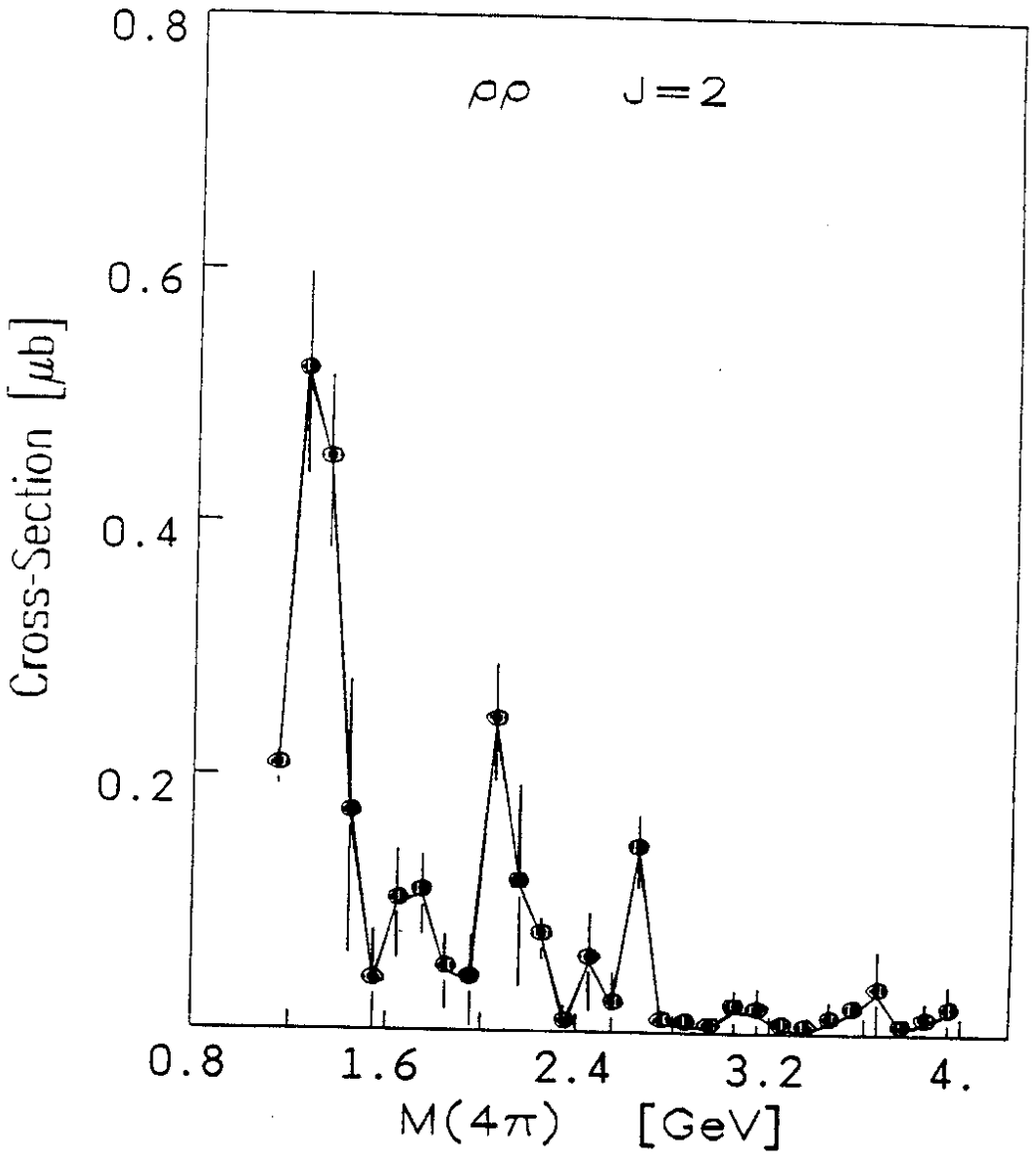

3e

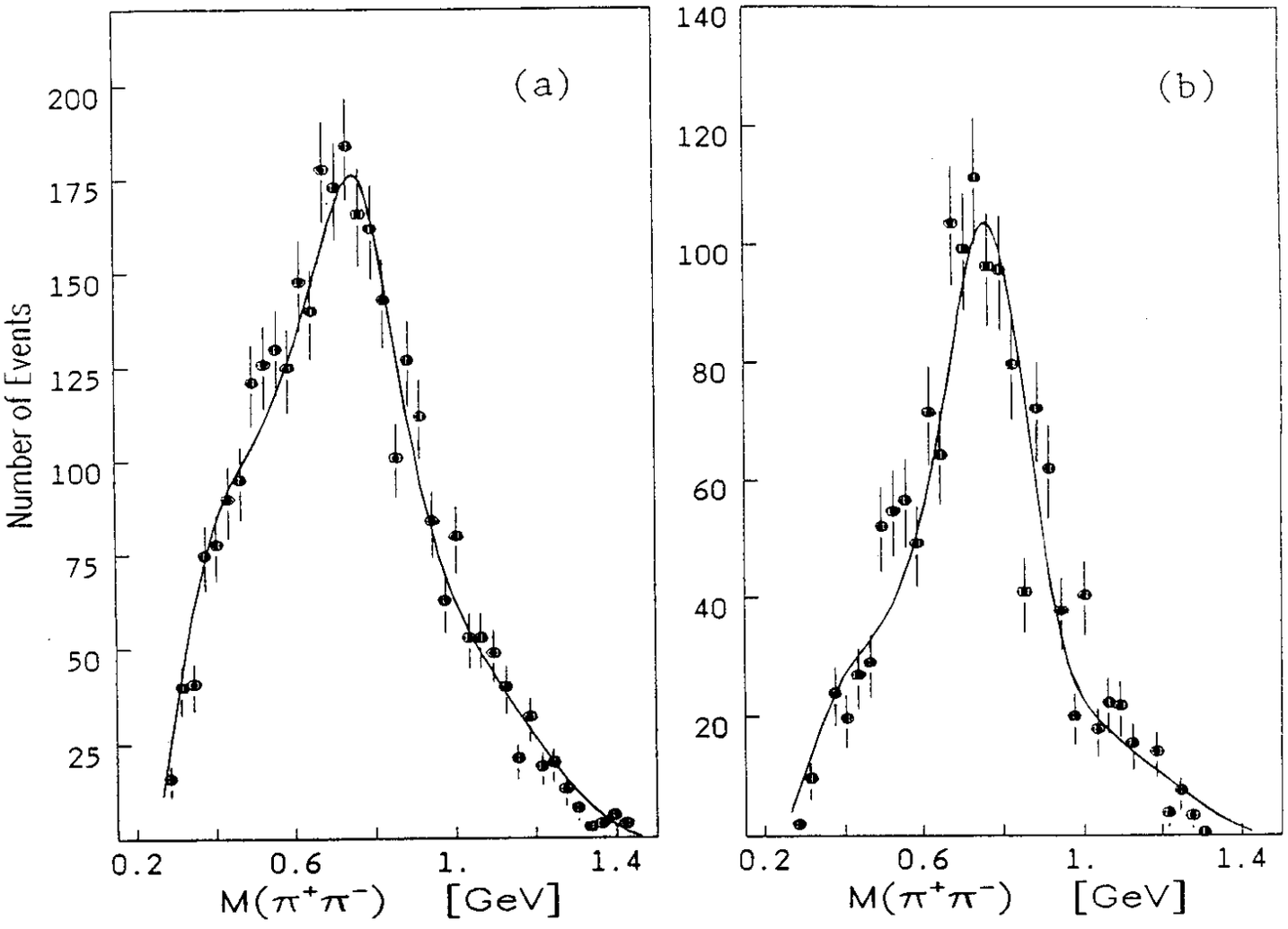
(a)
(b)
Number of Events
200
175
150
125
100
75
50
25
140
120
100
80
60
40
20
0.2
0.6
1.
1.4
M(π⁺π⁻) [GeV]

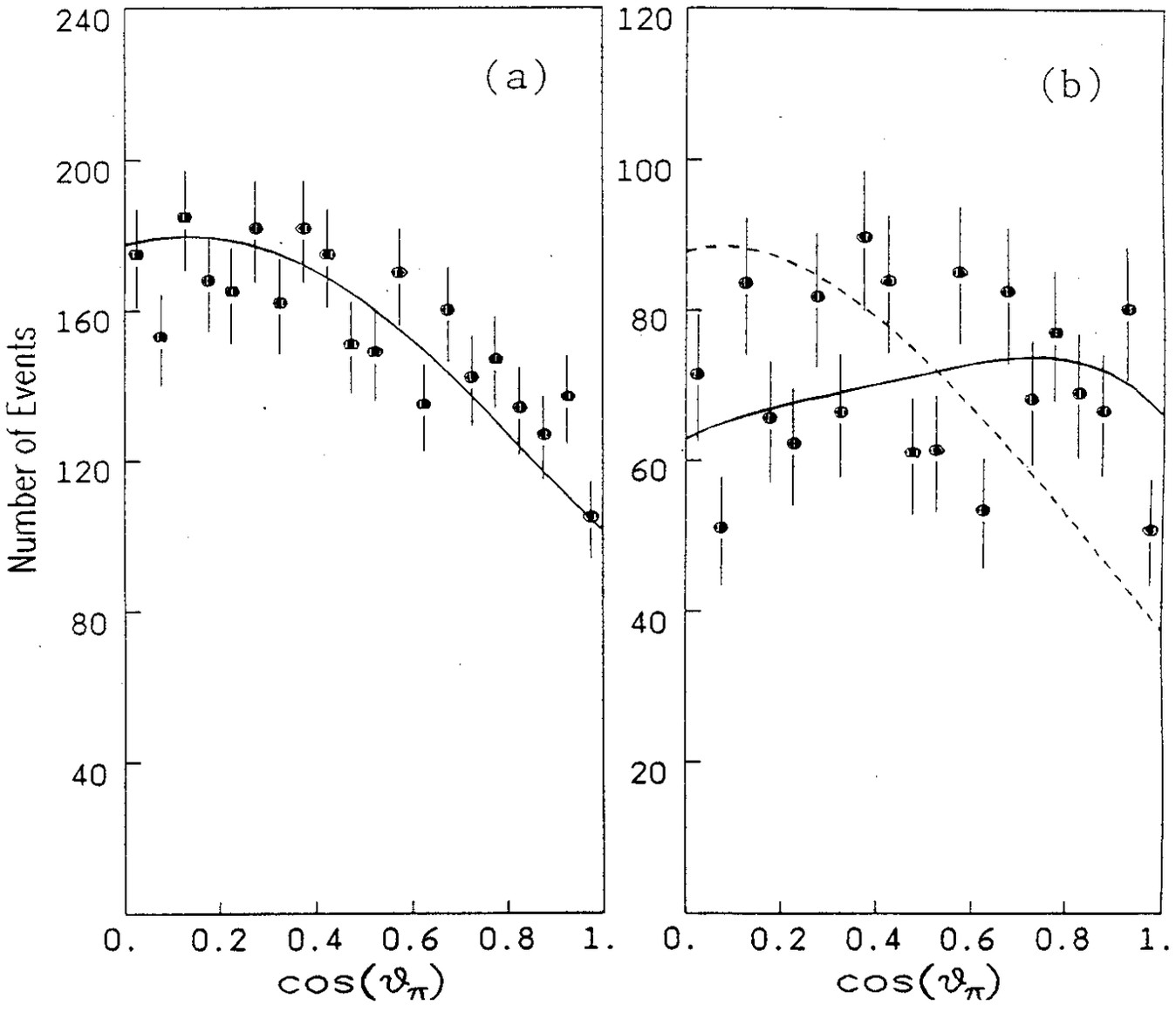
(a)
(b)
Number of Events
240
200
160
120
80
40
120
100
80
60
40
20
0.
0.2
0.4
0.6
0.8
1.
cos(ϑπ)

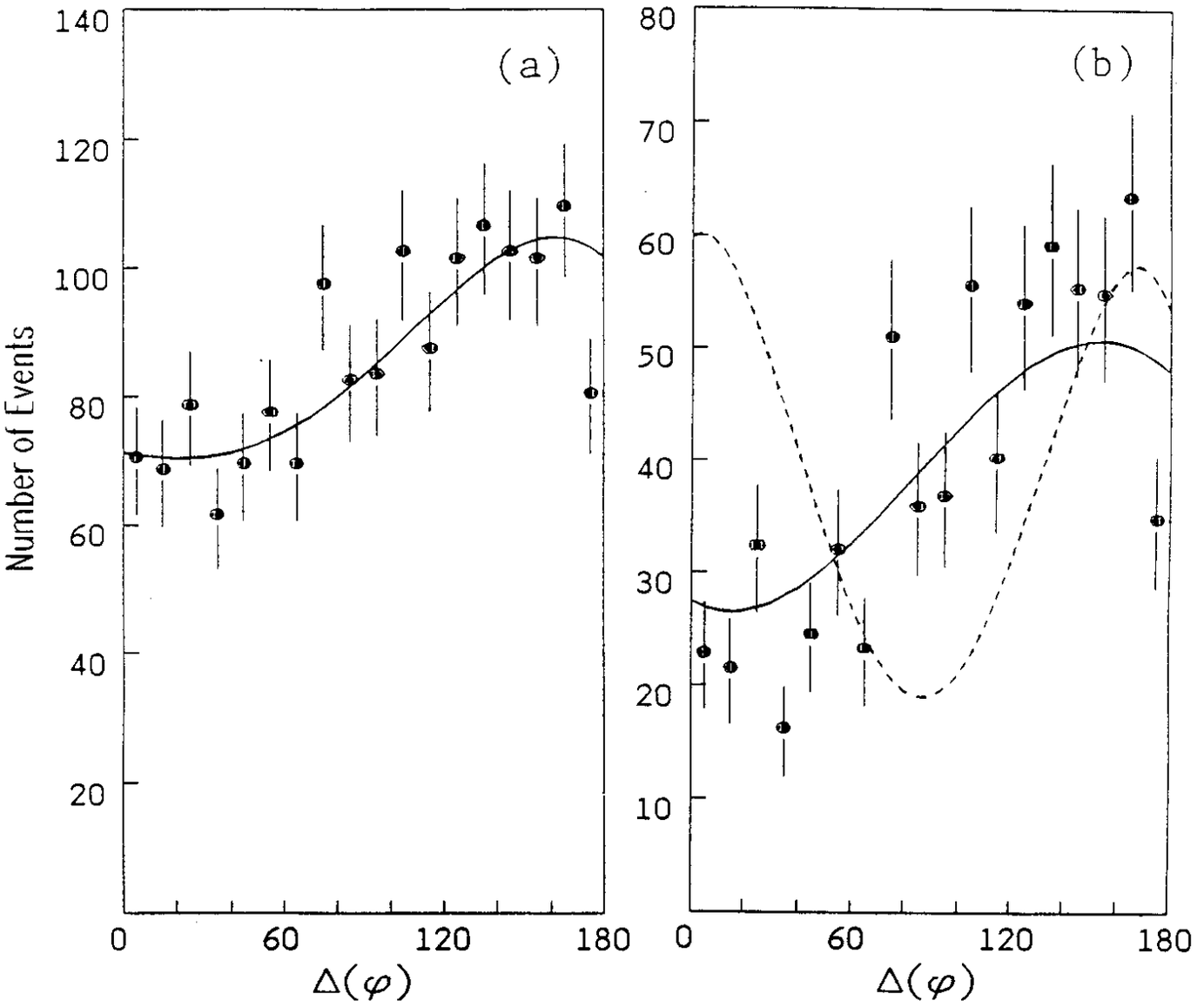
(a)
(b)
Number of Events
Δ(φ)
Δ(φ)
0
60
120
180
20
40
60
80
100
120
140
10
30
50
70